Available online at www.sciencedirect.com
ScienceDirect
Catalysis Today 120 (2007) 233–239
CATALYSIS TODAY
www.elsevier.com/locate/cattod

Liquid phase photooxidation of alcohol over niobium oxide without solvents

Tai Ohuchi, Toshiaki Miyatake, Yutaka Hitomi, Tsunehiro Tanaka *

Department of Molecular Engineering, Graduate School of Engineering, Kyoto University, Kyoto 615-8510, Japan

Available online 13 October 2006

Abstract

Photooxidation of alcohols without solvents in the presence of O_2 takes place at the atmospheric pressure and room temperature over niobium oxide. From the results of photooxidation of 1-pentanol over niobium oxides calcined at various temperatures, we judged that niobium oxide calcined at 773 K exhibits the highest activity and niobium oxides calcined at $\geq$873 K shows the higher selectivity to partial oxidation products than those calcined at $\leq$773 K. The reaction activity correlates to the BET specific surface area and crystallinity drawn from BET, TG-DTA, XRD and laser Raman measurements. The selectivity to partial oxidation products correlates to the amount of Lewis acid sites from FT-IR spectra of pyridine and NH_3 adsorbed niobium oxide catalysts, suggesting that Lewis acid sites play a role as an active site for total oxidation.

Keywords: Niobium oxide; Photocatalyst; Alcohol oxidation; Liquid phase; No solvents

1. Introduction

Alcohol oxidation to carbonyl compounds is one of the most important chemical transformations in the industrial chemistry. Carbonyl compound, ketones and aldehydes, are the precursors for many kinds of medicines, drugs, vitamins and fragrances and are also important intermediates for the variety of the complex syntheses [1]. However, toxic, corrosive, and expensive oxidants, stringent conditions such as high pressure and/or temperature, strong mineral acids are used in most of these reactions [2]. For example, alcohol oxidation is traditionally carried out in liquid phase by stoichiometric oxidants such as toxic and expensive chromium (VI) and manganese complexes, which produce a lot of heavy metal involving waste [1,2]. In addition, these reactions are often carried out in environmentally unfriendly organic solvents. Therefore, the development of catalytic methods for alcohol oxidation has been one of the most pursued targets in the last few years, due to substituting them with heterogeneous catalytic oxidation using clean and atom-efficient oxidants such as molecular O_2 and H_2O_2 without organic solvents [3–17].

Pillai and Demessie reported the oxidation of the primary alcohols and α,β-unsaturated alcohols using heterogeneous FeZSM-5 catalysts and H_2O_2 with high yield and selectivity. However, it involves the use of organic solvents such as methanol [5]. Uemura et al. reported Pd(II)-hydrotalcite-catalyzed alcohols oxidation [6,7]. This method requires the addition of pyridine as a ligand and toluene as a solvent. A recent study by Kaneda et al. proposed a method for selective oxidation of alcohols over hydroxyapatite-supported palladium nanoclusters [8,9]. The method also requires the presence of trifluorotoluene as a solvent. Although Wu et al. reported solvent free aerobic oxidation of alcohols by Pd/Al_2O_3 [10], the use of the noble metal such as Pd is essentially required.

In this context, photoreactions are promising processes and the development of photocatalysts is a subject that is now receiving much attention. TiO_2, which catalyzes oxidation of various organic compounds, is one example of practical and useful photocatalysts [11–17]. However, these reports were the oxidation of gas phase in high temperature [11], the oxidation of only lower alcohols [12–16] or the oxidation using solvents such as benzene [17] and

* Corresponding author. Tel.: +81 75 383 2559; fax: +81 75 383 2561.
E-mail address: tanakat@moleng.kyoto-u.ac.jp (T. Tanaka).

0920-5861/$ – see front matter
doi:10.1016/j.cattod.2006.07.044

the selectivity to partial oxidation products is low because of excess photoactivation of target products to lead to deep oxidation.

In this paper, photooxidation of alcohol in the presence of O_2 was examined at the atmospheric pressure and room temperature over various metal oxides without solvents. Niobium oxide showed higher reaction activity and the highest selectivity to partial oxidation products among various metal oxides. Here, we discuss the relationship between the catalytic activity and the physicochemical property of niobium oxide.

2. Experimental

2.1. Preparation of catalysts

Niobic acid, niobium oxide hydrate ($Nb_2O_5{\cdot}nH_2O$, AD/2872, HY-340), was kindly supplied from CBMM. Niobium oxide catalysts were prepared by calcinations of niobic acid in a dry air flow at 473–1073 K for 5 h. TiO_2 (P-25), ZrO_2 and Al_2O_3 were supplied from the Japan Catalysis Society (JRC-TIO-4, JRC-ZRO-1 and JRC-ALO-8). ZnO, MoO_3 and WO_3 were purchased from Nacalai Tesque. MgO and V_2O_5 were purchased from Merck Japan Ltd. $Ta_2O_5{\cdot}nH_2O$ was purchased from Mitsuwa Chemicals Co. Ltd. SiO_2 (CARiACT G-3) was offered from Fuji Silysia Chemical Ltd. These samples were calcined in a dry air flow at 773 K for 5 h. After calcinations, the catalysts were grinded into powder under 100 mesh.

2.2. Characterization of catalysts

The BET specific surface areas of catalysts were determined using N_2 adsorption isotherm at 77 K measured by a BELSORP 28SA. Simultaneous thermogravimetric and differential thermal analyses (TG-DTA) were performed on a Shimadzu DTG-50 thermal analyzer from room temperature (~298 K) to 1273 K at a heating rate of 10 K min^{-1} in a 40 ml min^{-1} flow of dried air. Crystal phase of each catalyst was determined by X-ray diffraction technique (XRD) under ambient conditions at room temperature using a Shimadzu XD-D1 X-ray diffractometer with Cu Kα radiation ($\bar{\lambda} = 1.5418$ Å). Laser Raman spectra were recorded under ambient conditions at room temperature. The laser Raman spectra were obtained with the 514.5 nm line of Ar^+ laser emission and an incident laser power of 100 mW and a resolution of 14.5 cm^{-1} using a JASCO NRS-2000. The FT-IR spectra of pyridine and NH_3 adsorbed samples were obtained using a Perkin-Elmer Spectrum One in a transmission mode. The 25 mg of sample was pressed into a self-supporting wafer and mounted in an *in situ* cell equipped with BaF_2 windows. The wafer was evacuated at 473 K for 1 h and treated by 80 Torr O_2 at 473 K for 2 h, followed by evacuation at 473 K for 1 h. Then, pyridine or NH_3 was adsorbed on the sample at 323 K. After adsorption, pyridine or NH_3 in the gas phase was removed completely by evacuation (10^{-6} Pa) at 323 K. The spectra were collected at 323 K.

2.3. The measurements of NH_3 chemisorption amount on niobium oxides

Before the NH_3 chemisorption measurement, niobium oxide sample was evacuated at 473 K for 1 h and was treated by 80 Torr O_2 at 473 K for 2 h, followed by evacuation at 473 K for 1 h. NH_3 was introduced to niobium oxides and the first adsorption (chemisorption and physisorption) isotherm was recorded at room temperature. After that, NH_3 was evacuated at for 30 min. Then the second NH_3 adsorption (physisorption) isotherm was recorded. The NH_3 chemisorption amount was determined by subtraction of the second isotherm from the first isotherm.

2.4. Catalytic reaction

The photocatalytic reaction was carried out in a quasi-flowing batch system at an atmospheric pressure. The reactor is similar to a Schrenck flask and made of Pyrex glass with a flat glass in the bottom. Metal oxide as a catalyst sample (100 mg) and 1-pentanol as a substrate (10 ml; Wako GR, 98.0%) were introduced to the reactor. In this study, no solvent was used. The catalyst was not evacuated nor pretreated in the presence of O_2. In addition, 1-pentanol was used without further purification. The suspension stirred by a magnetic stirrer at 323 K was irradiated from the flat bottom of the reactor through a reflection by a cold mirror with a 500 W ultrahigh-pressure Hg lamp (USHIO Denki Co.). Oxygen was flowed to the reactor at 2 cm^3 min^{-1} through 1-pentanol saturators. Organic products were analyzed by FID-GC and GC mass spectrometry. Further, at the down stream of the flow reactor, a trap filled with barium hydroxide solution ($Ba(OH)_2$) was equipped to determine the quantity of carbon dioxide (CO_2) as barium carbonate ($BaCO_3$).

3. Result and discussion

3.1. Photooxidation of 1-pentanol over various metal oxides

Table 1 shows the results of photooxidation of 1-pentanol over various metal oxides with molecular oxygen under irradiation at 323 K. The photogenerated products were pentanal (RCHO), pentanoic acid (RCOOH) and carbon dioxide (CO_2). No products was formed without metal oxide, Nb_2O_5, TiO_2 and ZnO showed higher activity among metal oxides. TiO_2 [11–17] and ZnO [18] were already known to be active for photooxidation of alcohols. Nb_2O_5 showed higher selectivity than TiO_2 at the same conversion level although TiO_2 showed higher activity than Nb_2O_5. No product was detected in the dark with niobium oxide. The evolution of pentanal and pentanoic acid responded to illumination. The reaction did not proceed under photoirradiation without catalyst. These results show that photooxidation of 1-pentanol over niobium oxide is a photocatalytic reaction. Niobium oxide catalyst was reusable and showed the same conversion and selectivity without any pretreatment as the catalyst as prepared.

Table 1
Photooxidation of 1-pentanol over various metal oxides

Sample	Reaction (time/h)	Products (mmol)			P.O.Sel.[c] (%)	PAL.Sel.[d] (%)	Conv.[e] (%)
		RCHO[a]	RCOOH[b]	CO_2			
Nb_2O_5	24	2.43	0.46	0.10	97	81	3.3
Nb_2O_5	84	4.38	7.74	0.88	93	34	14.1
Nb_2O_5	24[f]	Trace	0	Trace	–	–	–
TiO_2	24	2.85	5.92	1.80	83	27	11.7
ZnO	24	1.46	0.03	0.35	81	79	2.0
MgO	24	Trace	0	Trace	–	–	–
Al_2O_3	24	0.18	0.03	0.03	87	75	0.26
SiO_2	24	Trace	0	Trace	–	–	–
ZrO_2	24	0.23	0.06	Trace	93	74	0.34
V_2O_5	24	0.48	0.04	Trace	91	91	0.58
Ta_2O_5	24	0.11	0	Trace	89	92	0.14
MoO_3	24	Trace	0	Trace	–	–	–
WO_3	24	0.24	0	Trace	97	96	0.28
–[g]	24	0	0	Trace	–	–	–

[a] Pentanal.
[b] Pentanoic acid.
[c] Selectivity to partial oxidation products.
[d] Selectivity to pentanal.
[e] Conversion based on 1-pentanol.
[f] Reaction was carried out in the dark.
[g] Reaction was carried out without metal oxide.

3.2. Reaction and characterization of niobium oxide catalysts calcined at various temperatures

3.2.1. Photooxidation of 1-pentanol over niobium oxide catalysts calcined at various temperatures

Table 2 summarizes the results of BET specific surface area and photooxidation of 1-pentanol with molecular oxygen under irradiation at 323 K over niobic acid (uncalcined) and niobium oxide calcined at 473–1073 K. The BET specific surface area decreased with an increase in the calcination temperature. In particular, the BET specific surface area decreased drastically between 673 and 873 K. This abrupt change would be due to the formation of larger niobium oxide crystallites in the temperature range up to 773 K. The amount of pentanal and pentanoic acid production was increased gradually with the calcination temperature. At 773 K, 1-pentanol conversion and selectivity to partial oxidation products and pentanal were found to be 3.31%, 97% and 81%, respectively. Over niobium oxides calcined at $\geq$773 K, 1-pentanol conversion was decreased dramatically, and 1-pentanol conversion was 0.25% over niobium oxide calcined at 1073 K. Niobium oxide calcined at 773 K exhibited the highest activity in the photooxidation of 1-pentanol. We found higher selectivity to pentanal in niobium oxides calcined at 873–1073 K and decrease in conversion in proportion to a decrease in BET specific surface area in niobium oxide calcined at $\geq$773 K.

Table 2
Photooxidation of 1-pentanol over niobium oxides calcined at various temperatures[a]

Calcination temperature (K)	Sa[b] ($m^2\ g^{-1}$)	Products (mmol)			Select.[e] (%)	Select.[f] (%)	Conv.[g] (%)
		RCHO[c]	RCOOH[d]	CO_2			
Uncalcined	132	1.24	0.14	0.17	89	80	1.71
473	125	1.16	0.14	0.08	94	84	1.52
673	95	1.68	0.41	0.14	94	75	2.47
773	48	2.43	0.46	0.10	97	81	3.31
873	13	0.81	0.03	0.02	98	94	0.95
973	6	0.49	0.02	0.01<	98	94	0.58
1073	3	0.21	0.01	0.01<	96	91	0.25

[a] Reaction time; 24 h.
[b] BET specific surface area.
[c] Pentanal.
[d] Pentanoic acid.
[e] Selectivity to partial oxidation products.
[f] Selectivity to pentanal.
[g] Conversion based on 1-pentanol.

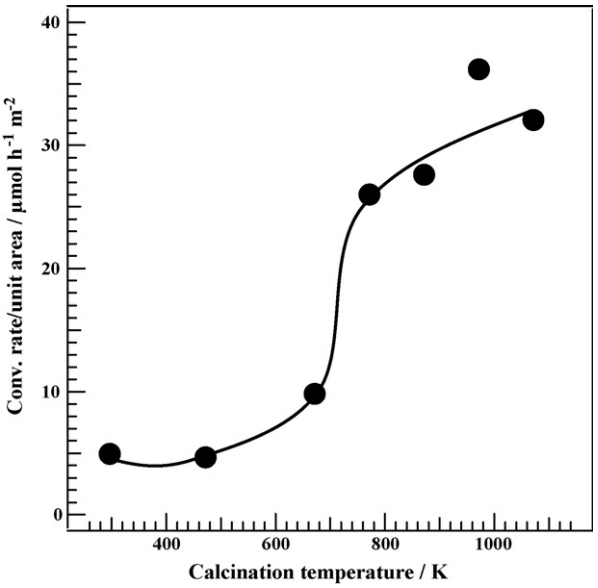

Fig. 1. Conversion rate per unit area over niobium oxide catalysts calcined various temperarures.

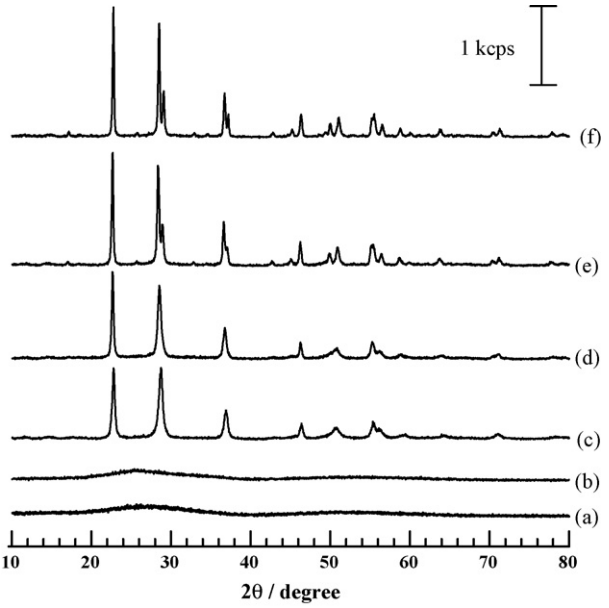

Fig. 3. XRD patterns of (a) niobic acid and niobium oxide catalysts calcined at (b) 673 K, (c) 773 K, (d) 873 K, (e) 973 K and (f) 1073 K.

Fig. 1 shows conversion rate per unit area over niobium catalysts calcined at various temperatures. One can notice that conversion rate per unit area is changed dramatically between 673 and 773 K. This suggests that intrinsic catalyst activity does not fall down but rises up at the temperature range.

3.2.2. TG-DTA curves, XRD patterns and Raman spectra of niobium oxide catalysts

Fig. 2 shows (A) TGA and (B) DTA curves of (a) niobic acid (uncalcined) and niobium oxides calcined at (b) 673 K and (c) 773 K. A weight loss (∼20 wt.%) was observed below 450 K and an endothermic peak was observed at 340 K in (a) niobic acid of TG-DTA curves, respectively. This is due to physical desorption of water. In the case of $Nb_2O_5{\cdot}nH_2O$ used as precursor, n is estimated to be approximately 3.5, no other weight loss was observed. A sharp exothermic peak was observed at 838 K in (a) niobic acid of DTA curve. This peak was observed in (b) and not in (c).

Fig. 3 shows the XRD patterns of niobium oxides calcined at various temperatures. The samples uncalcined and calcined at 673 K are amorphous. The samples calcined at 773 and 873 K involve TT-Nb_2O_5 with a pseudohexagonal structure. The samples calcined at 973 and 1073 K exhibit T-Nb_2O_5 with an orthorhombic structure [19–21]. XRD patterns of both the

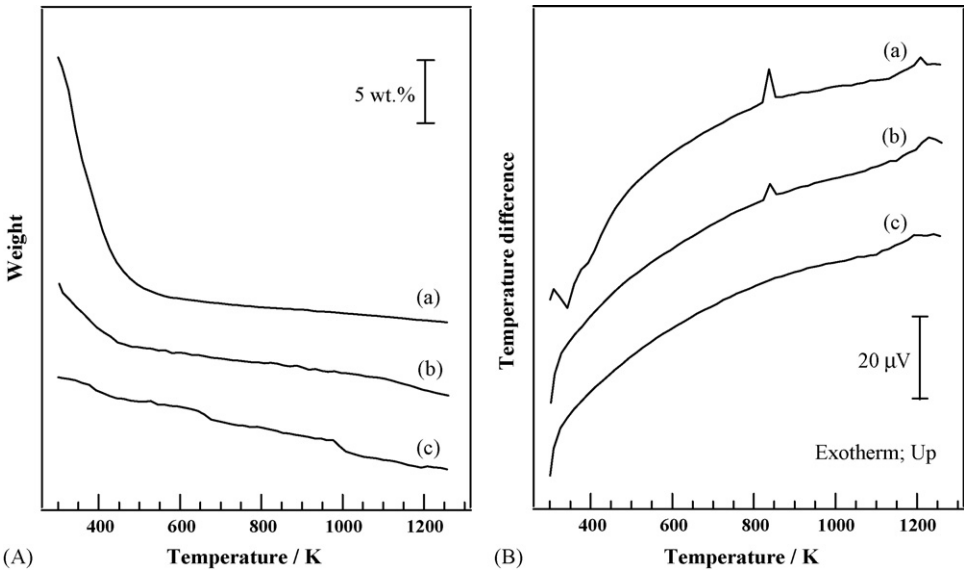

Fig. 2. (A) TGA and (B) DTA curves of (a) niobic acid and niobium oxide catalysts calcined at (b) 673 K and (c) 773 K.

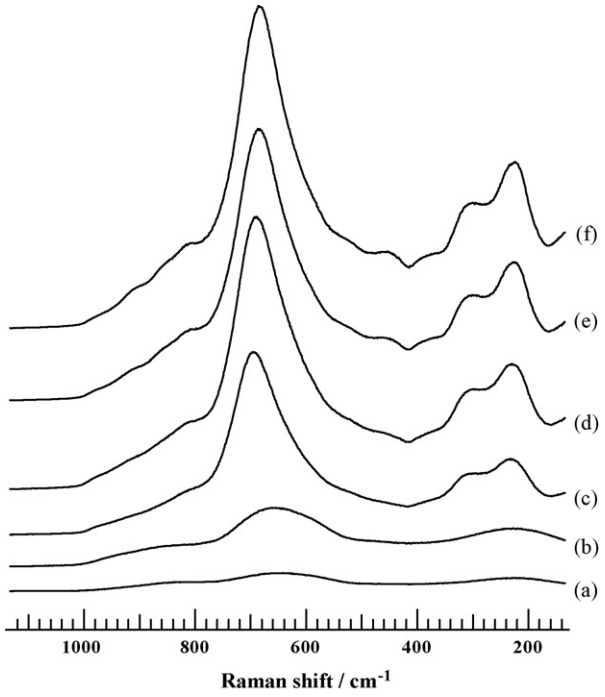

Fig. 4. Raman spectra of (a) niobic acid and niobium oxide catalysts calcined at (b) 673 K, (c) 773 K, (d) 873 K, (e) 973 K and (f) 1073 K.

phases are similar to each other with the slight shift of diffraction angles. But the closely spaced pair peaks at 28.53°, 29.09° and 36.75°, 37.22° are characteristic of the T-phase, while single peaks ($2\theta = 28.75°$, 36.93°) were formed in XRD patterns of the TT-phase. We found niobic acid is crystallized from amorphous to TT-Nb_2O_5 between 673 and 773 K and from TT-Nb_2O_5 to T-Nb_2O_5 between 873 and 973 K. The crystallization from amorphous to TT-Nb_2O_5 leads to decrease in the BET specific surface area drastically and the sharp exothermic peak at 838 K in DTA curves. The difference in temperature would be due to the difference in the condition of calcination. The crystallization also leads conversion rate per unit area to increase dramatically between 673 and 773 K. However, the difference of crystal between TT-Nb_2O_5 and T-Nb_2O_5 does not influence conversion rate per unit area. Crystallite sizes were estimated using Scherrer method. Crystallite sizes of niobium oxides calcined at 773, 873, 973 and 1073 K were 30, 50, 70 and 120 nm, respectively. Sintering is processed with an increase in calcination temperature.

To investigate the crystal phase near the surface, we carried out the Raman spectral measurement. Fig. 4 and Table 3 shows Raman spectra of niobium oxides calcined at various temperatures and the assignment [19,22]. For (a) niobic acid and (b) niobium oxide calcined at 673 K, broad and weak Raman bands were observed at ~900 and ~230 cm^{-1} as well as a broad and strong Raman band at ~640 cm^{-1}. These samples are amorphous. When (c) niobium oxide calcined at 773 K, the strong Raman band at ~640 cm^{-1} shifted to ~700 cm^{-1}. Raman bands in the low-wavenumber region (200–400 cm^{-1}) become more intense and better resolved than those of niobic acid and niobium oxide calcined at 673 K. This sample calcined at 773 K corresponds to TT-Nb_2O_5. The Raman features of niobium oxides calcined at (d) 873 K, (e) 973 K and (f) 1073 K were largely similar to those of (c) niobium oxide calcined at 773 K. However, additional weak Raman bands in the 400–500 cm^{-1} region and around 800 cm^{-1} were observed in niobium oxides calcined at (d) 873 K, (e) 973 K and (f) 1073 K as compared to (c) niobium oxide calcined 773 K. These samples calcined at 873, 973 and 1073 K correspond to T-Nb_2O_5. We found the difference in crystal phase between XRD pattern and Raman spectrum, TT-Nb_2O_5 (XRD) and T-Nb_2O_5 (Raman), about (d) niobium oxide calcined at 873 K. This indicates the phase transition from surface.

Table 4
NH_3 chemisorption amount of niobium oxide catalysts

Calcination temperature (K)	NH_3 chemisorption amount (μmol g^{-1})
473	776
673	569
773	278
873	56
973	33
1073	29

3.2.3. NH_3 chemisorption amount on niobium oxide catalysts

NH_3 chemisorption amount on niobium oxide catalysts was determined to evaluate the acidity. Table 4 shows NH_3 chemisorption amount on niobium oxides calcined at various temperatures. The amount of NH_3 chemisorption has a linear correlation to the BET specific surface area and decreases dramatically between 773 and 873 K. This decrease is probably caused by the phase transition of surface from TT-phase to T-phase. Masai et al. reported the effect of alkai promoters on Cu–Na–ZSM-5 catalysts in the benzyl alcohol oxidation [23]. Addition of alkali neutralizes the acid sites and causes a higher yield of the partial oxidation product and a low level of deep oxidation products. Niobium oxides calcined at ≤773 K have a lot of acid sites and lower selectivity to pentanal than the others.

Table 3
Assignment and Raman shift (cm^{-1}) obtained from Raman spectra

Assignment	Calcination temperature/K					
	Uncalcined	673	773	873	973	1973
Collinear ν(Nb–O–Nb)				805	797	805
ν_1(Nb–O)	642	655	697	689	687	686
Bridging ν_4(Nb–O–Nb)	230	226	302, 229	296, 229	301, 224	300, 224

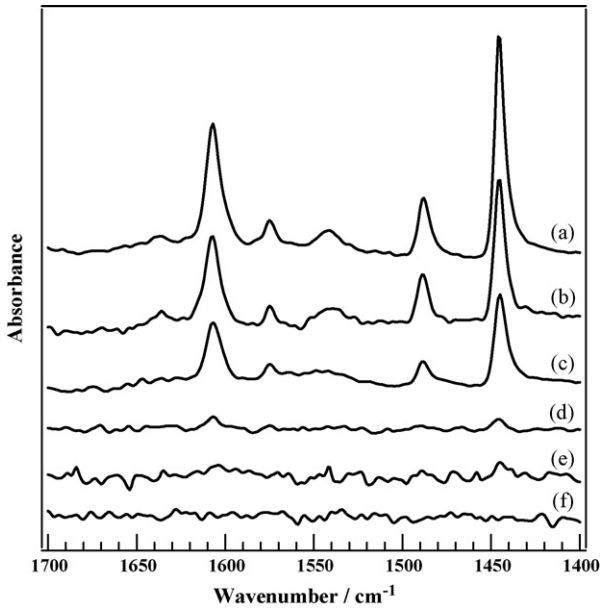

Fig. 5. FT-IR spectra of pyridine adsorbed niobium oxide catalysts calcined at (a) 473 K, (b) 673 K, (c) 773 K, (d) 873 K, (e) 973 K and (f) 1073 K.

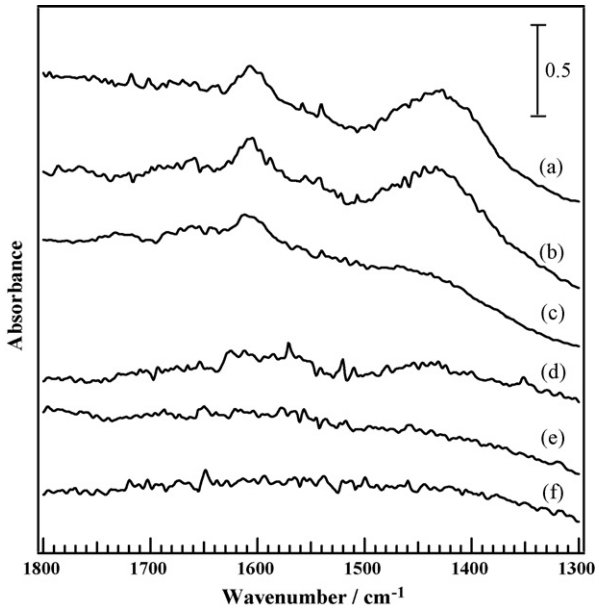

Fig. 7. FT-IR spectra of NH_3 adsorbed niobium oxide catalysts calcined at (a) 473 K, (b) 673 K, (c) 773 K, (d) 873 K, (e) 973 K and (f) 1073 K.

Therefore, acid sites may cause a deep oxidation also in 1-pentanol photooxidation over niobium oxide.

3.2.4. FT-IR spectra of pyridine and NH_3 adsorbed niobium oxide catalysts

The acidic characters of niobium oxides were determined by the FT-IR spectra of adsorbed pyridine and NH_3. Fig. 5 shows FT-IR spectra of pyridine adsorbed niobium oxides. Characteristic absorption at 1447 cm^{-1} is attributed to a coordinated pyridine meaning a pyridine adsorbed on Lewis acid site, and the adsorption at 1539 cm^{-1} is attributed to a pyridinium ion, a pyridine adsorbed on Brønsted acid site [24,25]. The Lewis acidity and the Brønsted acidity were evaluated as area of the FT-IR absorption bands in Fig. 6. The Lewis acidity decreased between 773 and 873 K. On the other hand, the Brønsted acidity decreased between 673 and 773 K. Taking into account that CO_2 selectivity dropped over the catalysts calcined at $\geq$773 K, these results suggest that Lewis acid sites cause a deep oxidation in 1-pentanol photooxidation. We also carried out the measurement of FT-IR spectra of adsorbed NH_3 to check the accuracy of acidity evaluated by pyridine adsorption since evaluation of Brønsted acidity is somewhat difficult. Fig. 7 shows FT-IR spectra of NH_3 adsorbed niobium oxides. Characteristic absorption at 1608 cm^{-1} is due to a NH_3 adsorbed on Lewis acid site, and the adsorption at 1438 cm^{-1} is due to a NH_3 adsorbed on Brønsted acid site [26,27]. The areas

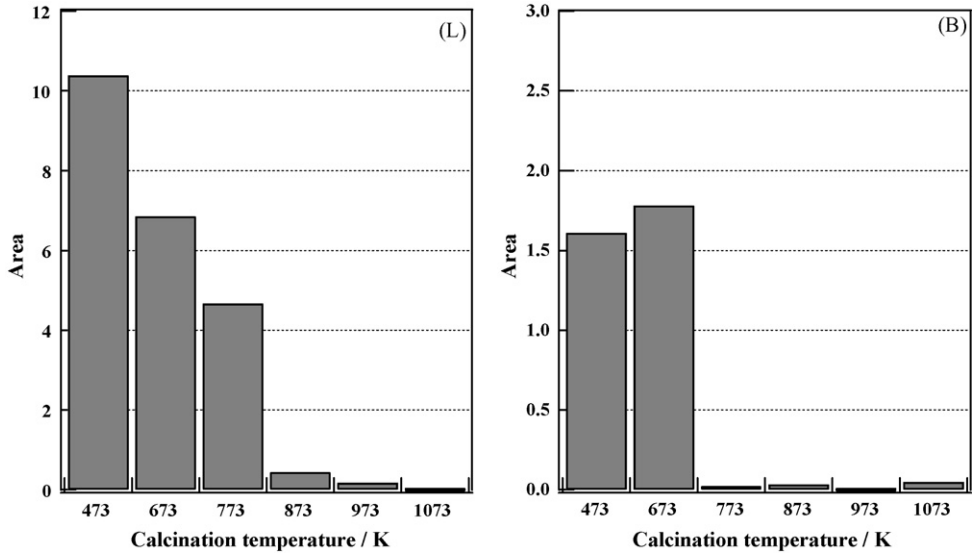

Fig. 6. Areas of (L) 1447 cm^{-1} and (B) 1539 cm^{-1} peaks of FT-IR spectra of pyridine adsorbed niobium oxide catalysts.

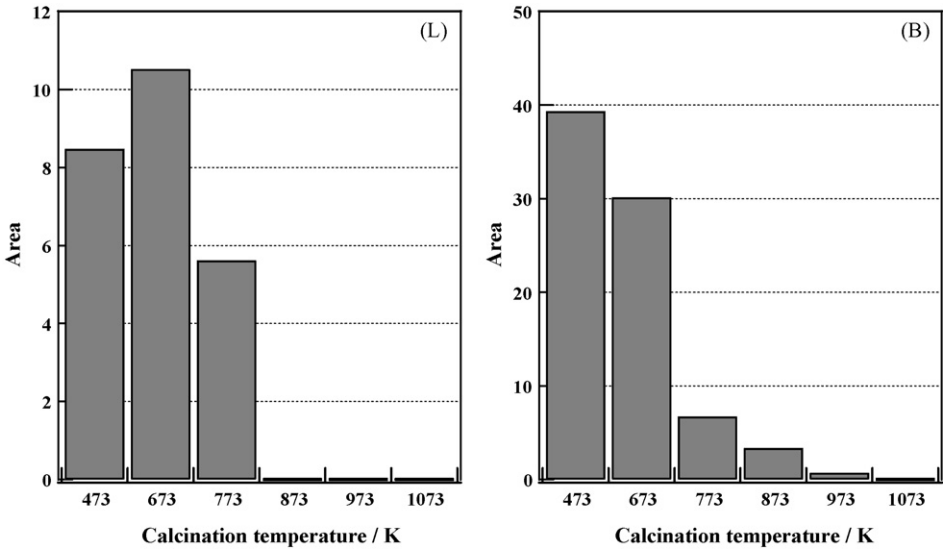

Fig. 8. Areas of (L) 1608 cm^{-1} and (B) 1438 cm^{-1} peaks of FT-IR spectra of NH_3 adsorbed niobium oxide catalysts.

of Lewis acidity and Brønsted acidity were evaluated in Fig. 8. The same results were obtained, suggesting that Lewis acid sites are responsible for deep oxidation of alcohol.

4. Conclusion

The photooxidation of 1-pentanol in liquid phase without solvents is performed over niobium oxide in an O_2-flowing batch system at the atmospheric pressure and room temperature. Niobium oxide exhibits the higher activity and highest selectivity to partial oxidation products among metal oxides. Niobium oxide calcined at 773 K exhibits the highest activity among those calcined at various temperatures. Conversion rate per unit area over niobium oxides calcined at $\geq$773 K is larger than those calcined at $\leq$673 K because niobium oxides calcined at $\geq$773 K have the crystal phase (TT-phase and T-phase). Selectivity to partial oxidation products is lower in niobium oxides calcined at $\leq$773 K because niobium oxides calcined at $\leq$773 K have a large amount of Lewis acid sites. The presence of Lewis acid sites promotes the deep oxidation. Acid sites influence the photocatalysis.

Acknowledgement

The present work is partially supported by the Grant-in-Aid for Scientific Research (KAKENHI) in Priority Area ''Molecular Nano Dynamics'' from Japan Ministry of Education, Culture, Sports, Science and Technology.

Reference

[1] R.A. Sheldon, J.K. Kochi, Metal-catalyzed Oxidations of Organic Compounds: Mechanistic Principles and Synthetic Methodology Including Biochemical Processes, 1981.
[2] R.C. Larock, Comprehensive Organic Transformations: A Guide to Functional Group Preparations, 1999.
[3] R.A. Sheldon, I.W.C.E. Arends, A. Dijksman, Catal. Today 57 (2000) 157.
[4] T. Mallat, A. Baiker, Chem. Rev. 104 (2004) 3037.
[5] N. Srinivas, V.R. Rani, M.R. Kishan, S.J. Kulkarni, K.V. Raghavan, J. Mol. Catal. A: Chem. 172 (2001) 187.
[6] N. Kakiuchi, T. Nishimura, M. Inoue, S. Uemura, Bull. Chem. Soc. Jpn. 74 (2001) 165.
[7] N. Kakiuchi, Y. Maeda, T. Nishimura, S. Uemura, J. Org. Chem. 66 (2001) 6620.
[8] K. Mori, K. Yamaguchi, T. Hara, T. Mizugaki, K. Ebitani, K. Kaneda, J. Am. Chem. Soc. 124 (2002) 11572.
[9] K. Mori, T. Hara, T. Mizugaki, K. Ebitani, K. Kaneda, J. Am. Chem. Soc. 126 (2004) 10657.
[10] H. Wu, Q. Zhang, Y. Wang, Adv. Synth. Catal. 347 (2005) 1356.
[11] U.R. Pillai, E.S. Demessie, J. Catal. 211 (2002) 434.
[12] J. Chen, D.F. Ollis, W.H. Rulkens, H. Bruning, Water Res. 33 (1999) 661.
[13] D.S. Muggli, J.T. Mccue, J.L. Falconer, J. Catal. 173 (1998) 470.
[14] D.S. Muggli, J.L. Falconer, J. Catal. 175 (1998) 213.
[15] J.L. Falconer, K.A.M. Bair, J. Catal. 179 (1998) 171.
[16] D.S. Muggli, K.H. Lowery, J.L. Falconer, J. Catal. 180 (1998) 111.
[17] F.H. Hussein, G. Pattenden, R. Rudham, J.J. Russell, Tetrahedron Lett. 25 (1984) 3363.
[18] J. Cunningham, B.K. Hodnett, J. Chem. Soc. Faraday Trans. 77 (1981) 2777.
[19] B. Orel, M. Maček, J. Grdadolnik, A. Meden, J. Solid State Electrochem. 2 (1998) 221.
[20] M. Ristić, S. Popović, S. Musić, Mater. Lett. 58 (2004) 2658.
[21] I. Nowak, M. Ziolek, Chem. Rev. 99 (1999) 3603.
[22] J.M. Jehng, I.E. Wachs, Chem. Mater. 3 (1991) 100.
[23] H. Hayashibara, S. Nishiyama, S. Tsuruya, M. Masai, J. Catal. 153 (1995) 254.
[24] M.I. Zaki, M.A. Hasan, F.A.A. Sagheer, L. Pasupulety, Colloids Surf. A: Physicochem. Eng. Aspects 190 (2001) 261.
[25] T. Hanaoka, K. Takeuchi, T. Matsuzaki, Y. Sugi, Catal. Today 8 (1990) 123.
[26] P. Concepción, P. Botella, J.M.L. Nietro, Appl. Catal. A 278 (2004) 45.
[27] G. Ramis, G. Busca, F. Bregani, P. Forzatti, Appl. Catal. 64 (1990) 259.